Applied Physics Letters

Defect-assisted sub-bandgap avalanche photodetection in interleaved carrier-depletion silicon waveguide for telecom band

Cite as: Appl. Phys. Lett. **104**, 091105 (2014); https://doi.org/10.1063/1.4867470
Submitted: 09 December 2013 . Accepted: 17 February 2014 . Published Online: 04 March 2014

Boris Desiatov, Ilya Goykhman, Joseph Shappir, and Uriel Levy

ARTICLES YOU MAY BE INTERESTED IN

Plasmonic silicon Schottky photodetectors: The physics behind graphene enhanced internal photoemission
APL Photonics **2**, 026103 (2017); https://doi.org/10.1063/1.4973537

Silicon-on-insulator waveguide photodetector with self-ion-implantation-engineered-enhanced infrared response
Journal of Vacuum Science & Technology A **24**, 783 (2006); https://doi.org/10.1116/1.2167975

Silicon waveguide-integrated optical power monitor with enhanced sensitivity at 1550nm
Applied Physics Letters **86**, 241103 (2005); https://doi.org/10.1063/1.1947379

Lock-in Amplifiers up to 600 MHz

AIP Publishing

© 2014 AIP Publishing LLC.

APPLIED PHYSICS LETTERS **104**, 091105 (2014)

Defect-assisted sub-bandgap avalanche photodetection in interleaved carrier-depletion silicon waveguide for telecom band

Boris Desiatov, Ilya Goykhman, Joseph Shappir, and Uriel Levy[a)]
Department of Applied Physics, The Benin School of Engineering and Computer Science, The Center for Nanoscience and Nanotechnology, The Hebrew University of Jerusalem, Jerusalem 91904, Israel

(Received 9 December 2013; accepted 17 February 2014; published online 4 March 2014)

This paper demonstrates on chip sub bandgap detection of light at 1550 nm wavelength using the configuration of interleaved PN junctions along a silicon waveguide. The device operates under reverse bias in a nearly fully depleted mode, thus minimizing the free carrier plasma losses and significantly increases the detection volume at the same time. Furthermore, substantial enhancement in responsivity is observed by the transition from reverse bias to avalanche breakdown regime. The observed high responsivity of up to 7.2 mA/W at 3 V is attributed to defect assisted photogeneration, where the defects are related to the surface and the bulk of the waveguide. © *2014 AIP Publishing LLC*.
[http://dx.doi.org/10.1063/1.4867470]

During the last decade, silicon photonics is considered as a key technology for miniaturization and on-chip monolithic integration of optical functionalities and systems.[1,2] Taking advantages of the well-established complementary metal-oxide-semiconductor (CMOS) fabrication process, a variety of integrated optical devices have been demonstrated in silicon, primarily on the basis of the silicon-on-insulator (SOI) platform. However, while silicon photodetectors are widely used in the visible spectral range, a defect-free bulk silicon cannot perform as an efficient absorber at telecom wavelengths (1.3 μm–1.6 μm) because the energy of infrared photons is not sufficient to overcome the energy bandgap of silicon (1.1 eV) and thus cannot photogenerate free carriers via interband transition. Over the years, the silicon photonics community developed solutions which allow the realization of silicon-based photodetectors operating in the telecom spectral band. Several photodetection mechanisms have been considered including the incorporation of germanium[3–7] or compound semiconductors[8,9] into silicon photonic circuitry by epitaxial growth or wafer bonding techniques, deposition of polycrystalline silicon active layer,[10] employing two-photon absorption process at high optical densities,[11–13] insertion of mid-bandgap defect states into silicon lattice to stimulate defect-mediated sub-bandgap absorption,[14–17] using defect states (surface and bulk) in PN junctions,[18,19] and using plasmonic structures to take advantage of the internal photoemission process.[20–24]

In parallel to the progress in developing silicon photodetectors for the telecom spectral band, nowadays, carrier-depletion optical modulator[25–30] is prevalently used in silicon photonics because of their higher modulation speed of majority carriers and lower power consumption compared with carrier injection optical modulators due to negligible leakage current of the diode operating in reverse bias. Recently, the concept of periodically interleaved PN junctions arrangement,[31–35] where the P- and the N-type regions of the diode alternate along the waveguide, was outlined and experimentally demonstrated for the construction of electro-optic silicon modulators. The distinctive improvement of this interleaved configuration compared to the lateral diode designs is associated with better light-carrier overlap and higher junction misalignment tolerance, because upon the application of reverse bias the depletion regions of the interleaved junctions are extended along the optical propagation direction rather than across the waveguide. As a result, the carrier depletion areas are greatly overlapped with the optical signal inside the waveguide and consequently contribute to higher modulation efficiency.

In this paper, we demonstrate defect-mediated near-infrared photodetection in silicon Mach-Zehnder carrier-depletion electro-optic modulator with periodic arrangement of PN junctions embedded into a submicron SOI waveguide. While this device was recently demonstrated for modulation applications,[35] here, we focus on its photodetection capabilities. In our presented device, the photodetection process takes place as light is propagating along the phase-shifter, providing power-monitoring functionality which is relying exclusively on the interleaved carrier-depletion modulator structure, with no need for additional fabrication steps. Additionally, we show that implementation of interleaved PN junction configuration for the construction of the phase shifter allows the operation of the device in a nearly fully depleted mode, which in turn significantly reduces the free carrier plasma losses within the waveguide. As a result, an optical signal propagating along the phase shifter is barely affected by the free carriers and thus can contribute to the photogeneration process, without decaying into un-desired loss channels. The combination of negligible free carriers' loss together with the fact that the vast majority of the fully depleted waveguide is available for photodetection increases the device photo-responsivity and makes the interleaved PN junctions design to be an attractive candidate for the construction of defect-mediated silicon photodetectors which are monolithically integrated with carrier-depletion modulators.

Our device is fabricated using SOI substrate with 250 nm thick silicon device layer on top of a 2 μm thick buried oxide. First, we apply a p-type base doping step by a single peak boron implantation through a thin (~20 nm) thermally grown

[a)]Author to whom correspondence should be addressed. Electronic mail: ulevy@mail.huji.ac.il

 © 2014 AIP Publishing LLC

silicon oxide layer for preventing channeling of light boron dopants. Next, the sample is annealed for 45 min at 1000°C. The optical structure of an asymmetric Mach-Zehnder interferometer (MZI) is defined by e-beam lithography (Raith 150 eLine) followed by 170 nm deep reactive ion etching of silicon (Oxford Plasmalab 100). The constructed 500 nm wide and 240 nm high silicon waveguide with a rib thickness of 70 nm supports a single transverse-electric (TE, in-plane) polarized optical mode. The periodically interleaved PN junctions were created in both arms of the MZI by electron beam lithography followed by phosphorus implantation through a 200 nm thick aluminum mask layer with following dopants drive at 1000°C. The actual boron and phosphorus doping concentrations after compensation were derived from 4-probe resistivity measurements and were found to be $\sim 4.3 \times 10^{17}\,\mathrm{cm}^{-3}$ and $\sim 4.1 \times 10^{17}\,\mathrm{cm}^{-3}$, respectively. The junctions spacing was estimated to be ~200 nm. Finally, ohmic contacts were formed by depositing and alloying aluminum electrodes on top of the highly doped silicon areas, which are located 1 μm away from the waveguide. Figures 1(a) and 1(b) show a schematic drawing of waveguide cross-section and the MZI, respectively. The misalignment of the interleaved mask for the phosphorus implantation in the transverse direction was found to be less that 50 nm and thus is not expected to perturb the operation of the device.

Optical transmission characterization of the fabricated devices was performed by butt coupling a TE polarized light from a tunable laser source (Agilent 81680A) and measuring the output optical power by InGaAs photodetector (Agilent 81634a). The transmission spectra were collected for different voltages with a maximal reverse bias of 3 V, corresponding to nearly fully depleted operation condition for which the maximal depletion region matches the physical junctions spacing of W = 200 nm. Figure 2(a) shows the measured normalized transmission spectra of an unbalanced (160 μm difference) MZI-modulator with a 1.4 mm long phase shifter in each arm. The relative phase shift $\Delta\phi$ as a function of the reverse bias was extracted from the transmission spectra by using the relation $\Delta\phi = 2\pi \times \Delta\lambda/FSR$, where $\Delta\lambda$ is the relative wavelength shift due to the application of reverse bias,

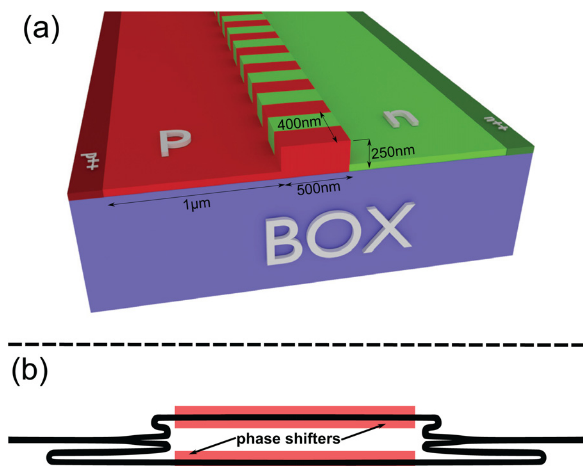

FIG. 1. (a) Schematics of the interleaved PN junctions. A rib like silicon waveguide is positioned on top of 2 μm thick buried oxide layer. (b) Schematics of the unbalanced Mach-Zehnder interferometer.

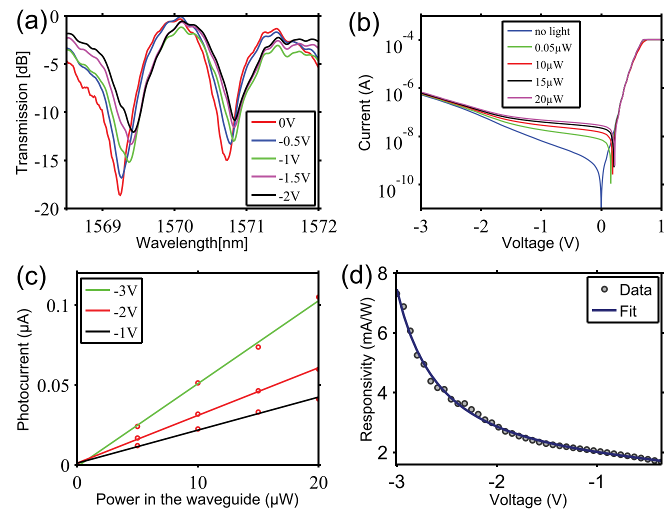

FIG. 2. (a) Normalized transmission spectrum measurements of a MZI-modulator with 1.4 mm long phase shifter operating under different values of reverse bias (typically the transmission spectrum is normalized to ~−35 dB, which is mostly the result of high in/out coupling loss to the chip). (b) I-V characteristics of the device for different incident optical power at operation wavelength of 1.55 μm. (c) Photocurrent versus optical power in one phase shifter of the Mach–Zehnder modulator. (d) Experimental responsivity-voltage dependence—the responsivity increases via avalanche multiplication gain in addition to square root dependence of the depletion layer.

and FSR is the free spectral range of the unbalanced MZI structure that was found to be 3.36 nm.

To experimentally demonstrate the reduction of the free carrier loss, when the device operates in nearly fully depleted mode, we performed the transmission measurements where the reverse bias was applied to both arms of the MZI. In this configuration, we anticipate a negligible change in the phase difference between the interferometer arms, while at the same time the transmission amplitude is expected to increase following the reduction of free carriers' concentration inside the waveguide. We measure the free carrier loss at zero bias to be 6 dB/cm and at −3 V bias (nearly fully depleted mode) to be 0.3 dB/cm.[35] Typical propagation loss of undoped waveguides is in the order of 2 dB/cm. Considering the application of photodetection, operating in a nearly fully depleted mode allows to employ even higher doping levels in the interleaved junctions compare to those used in the current work, followed by further reduction in junction width. This, in turn, could potentially increase the defect-mediated photogeneration process, while at the same time preserve low free carriers' absorption of the optical signal along the phase-shifter, which is essential for obtaining high efficiency detection. However, decreasing the junctions width is challenging from the perspective of fabrication.

The photo-detection capability of the device was tested by launching a TE polarized light around 1.55 μm wavelength and measuring its I-V characteristics at the presence of optical signal with varying powers (Figure 2(b)). We observed a linear increase (Figure 2(c)) of the current across the phase shifter with respect to the increase in optical power, where the slope of the curve corresponds to the responsivity of the phase-shifter according to $I_R = I_{dark} + R \times P_{in}$, where I_{dark} is the leakage current of the interleaved diode structure, R is the photodetector responsivity, and Pin is the optical power delivered to the phase shifter. In order to calculate the responsivity of

our device, we first estimated the amount of optical power arriving at the phase shifter. Taking into account ~17.5 dB coupling loss between the external tapered fiber and silicon bus waveguide (as it was measured by monitoring the output signal in the reference waveguide), a propagation loss (scattering + free carrier) of the bus waveguide in the order of 1 dB/mm, a 3 dB power splitting, and 1.5 dB loss in the Y-branch, we estimate the maximal optical power in the phase-shifter to be ~20 μW. Based on the I-V measurement results and the estimation of the input optical power, we plotted the device responsivity for different values of reverse bias, as shown in Figure 2(d). One could notice that the photodetector responsivity grows with the applied reverse bias. Moreover, the device photo-response shows an abrupt increase for reverse bias higher than 2 V. This behavior could be explained by avalanche multiplication of photogenerated free carriers inside the depletion region which is caused by the high electric field across the submicron scale PN junctions with junctions spacing of 200 nm. According to Figure 2(d), the measured responsivity is well fitted by the expression $R(V) \propto \sqrt{V_B - V} \times M$ (red line), where $M = \frac{1}{1-(V/V_{BD})^n}$ is the empiric relation for the avalanche multiplication process, V_B is the built-in voltage of the junction, V is the reverse bias, V_{BD} is the breakdown voltage, and n is typically varying between $2 < n < 6$. In our device, we obtained $V_{BD} = 3.5$ V and $n = 3$, with maximal responsivity of ~7.2 mA/W, corresponding to avalanche gain of ~7 compared to a photodetector without carrier multiplication process. It should be noted that using higher doping concentrations and smaller junctions spacing, which is favorable for achieving higher modulation efficiency in carrier-depletion interleaved electro-optic modulators,[35] may also provide higher multiplication gain and enhanced responsivity of photodetector due to the presence of stronger electric field across the diode with reduced junctions spacing.

Based on RC time constant optimization, our device was designed to support bandwidth of 23 GHz. This value was calculated from the simulated values of equivalent capacitance and serial resistance being 0.85 pF and 8.1 Ω, respectively. These parameters were experimentally tested by a small signal C-V measurement of the phase shifter together with the I-V device characterization. As shown in Figure 3(a), the measured value of the equivalent capacitance was found to be ~1 pF showing reasonable agreement with the simulation prediction. On the other hand, the serial resistance which was extracted from the slope of the I-V curve in forward bias around 1.5 V (Figure 3(b)) was found to be 330 Ω, far above the design expectation. The source of this high serial resistance was found to be the contact resistance, which is currently limited by our contact technology. It should be noted in this context that the high contact resistance is by no means an inherent characteristic of the interleaved PN junction detector presented in this paper. Contact resistance values in the range of few ohms are achievable with a standard CMOS silicide technology (e.g., Ref. 36) and will be implemented in the future to support tens gigahertz high speed operation regime.

Based on the measured serial resistance and capacitance, the 3 dB bandwidth of the device is expected to be ~0.48 GHz. To verify this prediction, we measured the small signal frequency response of our detector (Figure 4) by using a network analyzer and a commercial $LiNbO_3$ modulator as a reference. The measured 3 dB bandwidth was found to be around ~0.45 GHz, close to the value expected from the phase shifter capacitance and serial resistance characterizations. We could not observe any significant change in 3 dB bandwidth value as a function of applied voltage (gain), probably because the limiting factor is the contact resistance rather than the inherent properties of the detector.

In summary, we demonstrated the on chip sub bandgap detection of light at telecom wavelengths using the configuration of interleaved PN junctions along a silicon waveguide. The device operates under reverse bias in a nearly fully depleted mode, providing low free carrier plasma loss, and at the same time increases the detection volume. Additionally, significant enhancement in responsivity is obtained by the transition from reverse bias to avalanche breakdown regime. The observed high responsivity of up to 7.2 mA/W at 3 V is attributed to defect assisted photogeneration. While, in principle, these defects are located both in the bulk and in the surface, we believe that surface states are playing a dominant role in the process, due to the fact that the silicon waveguide is exposed rather than being passivated by thermal oxide. For structures which are covered by plasma enhanced chemical vapor deposition oxide, no significant modification in surface states is expected,[37] and thus we do not anticipate a significant change in the responsivity of the device. The responsivity of our detector can be further improved by choosing a higher doping level and decreasing the period of

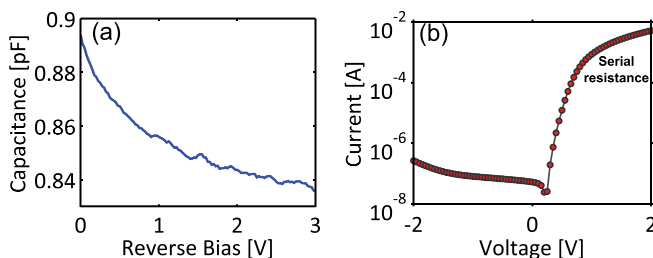

FIG. 3. (a) Small signal differential capacitance measurement of 1.4 mm long interleaved phase shifter. (b) Electrical current-voltage characterization of 1.4 mm long interleaved phase shifter.

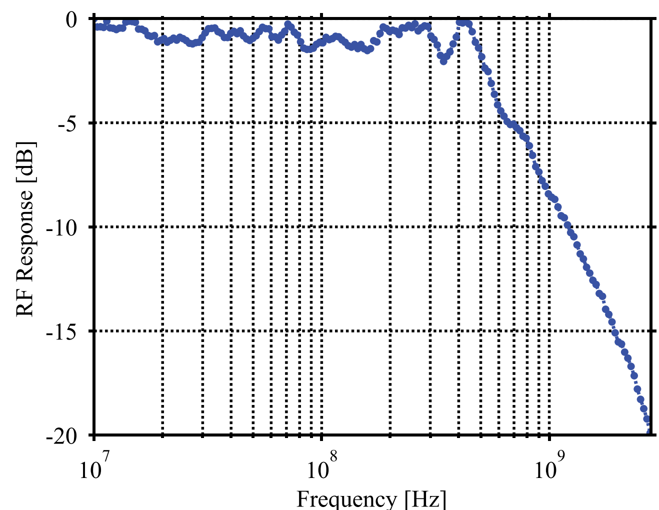

FIG. 4. RF response of the detector at −1 V applied voltage.

the interleaved junction. Furthermore, considering the low absorption of the optical signal in our structure, the responsivity can be further enhanced either by using a longer phase shifter or by using a cavity which allows the light to cross the structure several times.

The authors acknowledge technical support from Noa Mazurski. The research was supported in parts by the U.S.-Israel Binational Science Foundation, the TERASANTA Consortium, and the Focal Technology Area on Nanophotonics for Detection. B.D. and I.G. acknowledge the Eshkol fellowship from the Israeli Ministry of Science and Technology. The devices were fabricated at the Center for Nanoscience and Nanotechnology, The Hebrew University of Jerusalem.

[1]M. Streshinsky, R. Ding, Y. Liu, A. Novack, C. Galland, A. E. Lim, P. Guo-Qiang Lo, T. Baehr-Jones, and M. Hochberg, Opt. Photonics News **24**, 32–39 (2013).
[2]B. Jalali and S. Fathpour, J. Lightwave Technol. **24**, 4600 (2006).
[3]C. T. DeRose, D. C. Trotter, W. A. Zortman, A. L. Starbuck, M. Fisher, M. R. Watts, and P. S. Davids, Opt. Express **19**, 24897 (2011).
[4]L. Tang, S. E. Kocabas, S. Latif, A. K. Okyay, D.-S. Ly-Gagnon, K. C. Saraswat, and D. A. B. Miller, Nat. Photonics **2**, 226 (2008).
[5]Y. Kang, H.-D. Liu, M. Morse, M. J. Paniccia, M. Zadka, S. Litski, G. Sarid, A. Pauchard, Y.-H. Kuo, H.-W. Chen *et al.*, Nat. Photonics **3**, 59 (2009).
[6]S. Assefa, F. Xia, and Y. A. Vlasov, Nature **464**, 80 (2010).
[7]L. Chen, P. Dong, and M. Lipson, Opt. Express **16**, 11513 (2008).
[8]H. Park, A. W. Fang, R. Jones, O. Cohen, O. Raday, M. N. Sysak, M. J. Paniccia, and J. E. Bowers, Opt. Express **15**, 6044 (2007).
[9]S. Feng, Y. Geng, K. M. Lau, and A. W. Poon, Opt. Lett. **37**, 4035 (2012).
[10]K. Preston, Y. H. Lee, M. Zhang, and M. Lipson, Opt. Lett. **36**, 52 (2011).
[11]T. K. Liang, H. K. Tsang, I. E. Day, J. Drake, A. P. Knights, and M. Asghari, Appl. Phys. Lett. **81**, 1323 (2002).
[12]R. Hayakawa, N. Ishikura, H. C. Nguyen, and T. Baba, Appl. Phys. Lett. **102**, 031114 (2013).
[13]H. Chen and A. W. Poon, Appl. Phys. Lett. **96**, 191106 (2010).
[14]A. P. Knights, J. D. B. Bradley, S. H. Gou, and P. E. Jessop, J. Vac. Sci. Technol., A **24**, 783 (2006).
[15]Y. Liu, C. W. Chow, W. Y. Cheung, and H. K. Tsang, IEEE Photonics Technol. Lett. **18**, 1882 (2006).
[16]J. K. Doylend, P. E. Jessop, and A. P. Knights, Opt. Express **18**, 14671 (2010).
[17]R. R. Grote, K. Padmaraju, B. Souhan, J. B. Driscoll, K. Bergman, and R. M. Osgood, IEEE Photonics Technol. Lett. **25**, 67 (2013).
[18]H. Yu, D. Korn, M. Pantouvaki, J. Van Campenhout, K. Komorowska, P. Verheyen, G. Lepage, P. Absil, D. Hillerkuss, L. Alloatti *et al.*, Opt. Lett. **37**, 4681 (2012).
[19]Y. Li, S. Feng, Y. Zhang, and A. W. Poon, Opt. Lett. **38**, 5200 (2013).
[20]A. Akbari and P. Berini, Appl. Phys. Lett. **95**, 021104 (2009).
[21]M. Casalino, M. Iodice, L. Sirleto, I. Rendina, and G. Coppola, Opt. Express **21**, 28072 (2013).
[22]S. Zhu, H. S. Chu, G. Q. Lo, P. Bai, and D. L. Kwong, Appl. Phys. Lett. **100**, 061109 (2012).
[23]A. Sobhani, M. W. Knight, Y. Wang, B. Zheng, N. S. King, L. V. Brown, Z. Fang, P. Nordlander, and N. J. Halas, Nat. Commun. **4**, 1643 (2013).
[24]I. Goykhman, B. Desiatov, J. Khurgin, J. Shappir, and U. Levy, Opt. Express **20**, 28594 (2012).
[25]Q. Xu, B. Schmidt, S. Pradhan, and M. Lipson, "Micrometre-scale silicon electro-optic modulator," Nature **435**, 325–327 (2005).
[26]W. M. Green, M. J. Rooks, L. Sekaric, and Y. A. Vlasov, Opt. Express **15**, 17106 (2007).
[27]H. C. Nguyen, Y. Sakai, M. Shinkawa, N. Ishikura, and T. Baba, Opt. Express **19**, 13000 (2011).
[28]A. Liu, L. Liao, D. Rubin, H. Nguyen, B. Ciftcioglu, Y. Chetrit, N. Izhaky, and M. Paniccia, Opt. Express **15**, 660 (2007).
[29]P. Dong, S. Liao, D. Feng, H. Liang, D. Zheng, R. Shafiiha, C.-C. C. Kung, W. Qian, G. Li, X. Zheng *et al.*, Opt. Express **17**, 22484 (2009).
[30]D. J. Thomson, F. Y. Gardes, Y. Hu, G. Mashanovich, M. Fournier, P. Grosse, J. M. Fedeli, and G. T. Reed, Opt. Express **19**, 11507 (2011).
[31]Z.-Y. Li, D.-X. Xu, W. R. McKinnon, S. Janz, J. H. Schmid, P. Cheben, and J.-Z. Yu, Opt. Express **17**, 15947 (2009).
[32]M. Ziebell, D. Marris-Morini, G. Rasigade, P. Crozat, J.-M. Fédéli, P. Grosse, E. Cassan, and L. Vivien, Opt. Express **19**, 14690 (2011).
[33]H. Xu, X. Xiao, X. Li, Y. Hu, Z. Li, T. Chu, Y. Yu, and J. Yu, Opt. Express **20**, 15093 (2012).
[34]J. C. Rosenberg, W. M. J. Green, S. Assefa, D. M. Gill, T. Barwicz, M. Yang, S. M. Shank, and Y. A. Vlasov, Opt. Express **20**, 26411 (2012).
[35]I. Goykhman, B. Desiatov, S. Ben-Ezra, J. Shappir, and U. Levy, Opt. Express **21**, 19518 (2013).
[36]D. X. Xu, S. R. Das, C. J. Peters, and L. E. Erickson, Thin Solid Films **326**, 143 (1998).
[37]G. Dingemans, M. M. Mandoc, S. Bordihn, M. C. M. van de Sanden, and W. M. M. Kessels, Appl. Phys. Lett. **98**, 222102 (2011).